Universality of intermittent convective transport in the scrape-off layer of magnetically confined devices

Ghassan Y. Antar, Glenn Counsell, Yang Yu, Brian Labombard, and Pascal Devynck

Citation: Phys. Plasmas **10**, 419 (2003); doi: 10.1063/1.1536166
View online: http://dx.doi.org/10.1063/1.1536166
View Table of Contents: http://pop.aip.org/resource/1/PHPAEN/v10/i2
Published by the American Institute of Physics.

Universality of intermittent convective transport in the scrape-off layer of magnetically confined devices

Ghassan Y. Antar
Fusion Energy Research Program, University of California San Diego, 9500 Gilman Drive, La Jolla, California 92093-0417

Glenn Counsell
EURATOM/UKAEA Fusion Association, Culham Science Centre, Abingdon, Oxfordshire OX14 3DB, United Kingdom

Yang Yu
Institute of Plasma Physics, Hefei, 230031, People's Republic of China

Brian Labombard
Massachusetts Institute of Technology, Cambridge, Massachusetts 02139

Pascal Devynck
Association Euratom-CEA, CEA/Cadarache, 13108 St-Paul-Lez-Durance Cédex, France

(Received 16 August 2002; accepted 11 November 2002)

The nature of intermittency, long observed in magnetic fusion devices, was revisited lately [G. Antar *et al.*, Phys. Rev. Lett. **87**, 065001 (2001)]. It was shown that intermittency is caused by large-scale events with high radial velocity reaching about 1/10th of the sound speed. These type of structures were named ''avaloids.'' In the present article, the universality of convective turbulence in magnetically confined plasmas is investigated. Turbulence properties in the scrape-off layer of four different magnetic fusion devices are compared. Namely, the Tore Supra tokamak [Tore Supra Team, Nuclear Fusion, **40**, 1047 (2000)] with circular cross-section limiter-bounded plasma, the Alcator C-Mod tokamak [B. LaBombard *et al.*, Phys. Plasmas **8**, 2107 (2001)] which is a divertor device, the Mega-Ampere Spherical Tokamak (MAST) [A. Sykes *et al.*, Phys. Plasmas **8**, 2101 (2001)] with vacuum chamber walls far from the plasma last closed flux surface and the PISCES linear plasma device [D. Geobel *et al.*, Rev. Sci. Istrum. **56**, 1717 (1985)]. The statistical properties of the turbulent signals in the four devices are found to be identical allowing us to conclude that intermittent convective transport by avaloids is universal in the sense that it occurs and has the same properties in many confinement devices with different configurations. © *2003 American Institute of Physics.* [DOI: 10.1063/1.1536166]

I. INTRODUCTION

Turbulence in the scrape-off layer (SOL) of magnetically confined plasmas has long been reported to be intermittent (see, for example, Refs. 1–5). The nature of this transport was revisited recently in Refs. 6 and 7, where it was shown that the intermittent structures are convective in nature, with a high radial velocity reaching about 1/10th of the sound speed. Avaloids were thus defined as large-scale coherent concentration of plasma that are encountered intermittently in the SOL having high radial velocities. They are responsible for the intermittent convective transport leading to plasma in the SOL that exists in a discontinuous fashion as it is intermittent. It was also shown that, even though they may occupy less than 20% of the total duration of the signal, they account for about 50% of the radial transport near the last closed flux surface. In the far SOL, and because turbulent diffusion is nearly absent, intermittent convective transport accounts for the totality of the plasma that survived parallel transport.

The main contribution of this article is to emphasize the universality of intermittent convective transport by avaloids. We compare the fluctuations properties for different confinement devices, and provide experimental evidence that the fluctuations properties are identical in various aspects. To achieve our purpose, we compare the raw signals, the probability distribution functions (PDF's), the power spectrum and the conditional averaging results from which one can deduce the velocities and the spatial length scales of avaloids.

Intermittent convective transport leads to hot plasma in contact with the chamber first wall even when the latter is far from the last closed flux surface (LCFS). Exponential, or nearly-exponential, density decay often exists near the LCFS,[8] but in the far SOL, the fast intermittent convective transport tends to flatten the profile. Consequently, the SOL is a region extending up to the vacuum vessel walls of open field lines where turbulence dynamics are still complex and highly intermittent. We have shown in the PISCES linear device, that plasma extends up to the wall located at 10 cm away from the plasma center, that is, at 4 times the plasma radius equal to 2.5 cm. It will be shown hereafter that plasma is detected as far as 30 cm away from the LCFS in the MAST spherical tokamak. In Alcator C-MOD, avaloids lead

to a flattening of the density profiles which can more naturally be reproduced using a model based on a convective *ansatz* (the time-averaged particle flux density proportional to the local time-averaged density) than by a diffusive model where the time-averaged particle flux density is proportional to the radial derivative of the local time-averaged density.[5]

The SOL width is crucial to all plasma-facing components study and evaluation. The fact that fast intermittent convective transport carries not only matter but also heat may lead to the enhanced erosion observed in many magnetically confined devices.[9] The average density and temperature that can be deduced from swept Langmuir probes underestimate the instantaneous values of the plasma density and temperature in the SOL. The existence of a threshold, above which physical sputtering by ions occurs, makes the role of avaloids in enhancing the sputtering even more crucial; this sputtering is not continuous but rather intermittent.

Another rather important subject affected by the avaloids existence is the understanding of the Bohm vs gyro-Bohm scaling of the heat and particle transport as a function of ρ/a, where ρ and a are, respectively, the ion Larmor and plasma minor radii.[10] The existence of large-scale events with high radial velocity that dominates the transport, may in fact be the origin of the observed gyro-Bohm scaling where the particle confinement time does not depend on ρ/a. The reason behind this can be summarized as follows. Assume that the average radial velocity scales like $V_r = c_s(\rho/a)$ and the effective particle diffusion coefficient like $D = D_B(\rho/a) = \rho c_s(\rho/a)$; the subscript B denotes the Bohm-type. Then, for the particle confinement time (τ) two cases can emerge:

Diffusion dominated transport (Bohm)

$$\tau_D = a^2/D = \frac{a^2}{D_B}(a/\rho),$$

Convection dominated transport (gyro−Bohm)

$$\tau_V = a/V_r = \frac{a^2}{D_B}.$$

Accordingly, and assuming that some link exists between core and edge turbulence, convective large-scale transport events such avaloids can provide an explanation of why experimental data does not scale like Bohm.

As it has been shown in Ref. 7, plasma density in the far SOL can attain momentarily the same values as inside the last closed flux surface. Hence, avaloids strongly affect the fluctuations measured by reflectometry at the plasma edge, where the equivalence between time-of-flight and density becomes no longer valid. High densities in the SOL can lead to very low signals even when the reflectometer is probing the region inside the plasma but close to the LCFS.

The purpose of this article is to investigate the question of universality that we briefly exposed in Ref. 7 by comparing the turbulence properties in the SOL of PISCES and Tore Supra, two very different plasma devices. To accomplish our purpose, we compare the properties of turbulence in the scrape-off layer of four different magnetic fusion devices, that are, Alcator C-MOD, MAST, Tore Supra, and PISCES. We use mainly the ion saturation current recorded by Langmuir probes for this comparison. It is shown that the turbulent fluctuations from the statistical point of view are identical for the four devices. The rest of this paper is organized as follows. In the next section, we describe briefly the four devices and the experimental conditions under which the data were taken. Moreover, we describe the different configurations of the Langmuir probes, which change from very small in PISCES to relatively large and perturbative in Tore Supra. In Sec. III, we compare the raw signals and their histograms. In Sec. IV, we show that the power spectra of the four devices is composed of one scaling region with a scaling exponent about -1.6. The similarity of the average asymmetric shape of avaloids is demonstrated in Sec. V as well as the similarity among the histograms of the time between two events. Finally, and before concluding, we determine the spatial length scales of avaloids and their velocities.

II. THE EXPERIMENTAL SETUPS

This section describes rather briefly the four plasma confinement devices that are used in our comparison of the SOL turbulence properties. The differences among the four devices will be highlighted to support our claim that the existence of avaloids is universal. We also describe the different Langmuir probes architecture and dimensions in order to emphasize that the statistical properties of the signals do not depend on the probe configuration. We recall that the four machines are: the Tore Supra tokamak, the Alcator C-Mod tokamak, the MAST spherical Torus, and the PISCES linear plasma device.

A. The Tore Supra tokamak

Tore Supra is a tokamak with minor radius about $a = 76$ cm and a major radius equal to $R = 2.25$ m.[11] The cross section of the plasma is circular and a limiter separates the core plasma from the walls. The L-mode plasma conditions under which the Langmuir probe measurements were taken are: Toroidal magnetic field 1.5 T, plasma current 1 MA, and the average plasma density about 4×10^{19} m^{-3} (see Ref. 6 for more details).

The reciprocating Langmuir probe is installed on the top of the Tore Supra tokamak.[12] The tips configuration is illustrated in Fig. 1(a). They are composed of two sets of three composite carbon tips with 0.6 cm of diameter toroidally separated by a distance of 2 cm. The poloidal separation among the tips is 0.68 cm. The tips are shielded from the plasma by a 3 cm diam cylinder with six holes drilled through it. The radius of the holes is 4 mm in diameter defining the collection area. The tips are biased to -100 V with respect to the vessel ground and is verified to yield a probe current in the ion saturation current. The probe goes into the plasma to a predetermined position and returns in about 150 ms. Several plunges are performed during each discharge and 8000 data points are recorded at a rate of 1 MHz. Data sets where the probe is nearly motionless with respect to the LCFS are selected. The distance to the last closed flux surface is chosen to be equal to 1.5 ± 0.5 cm.

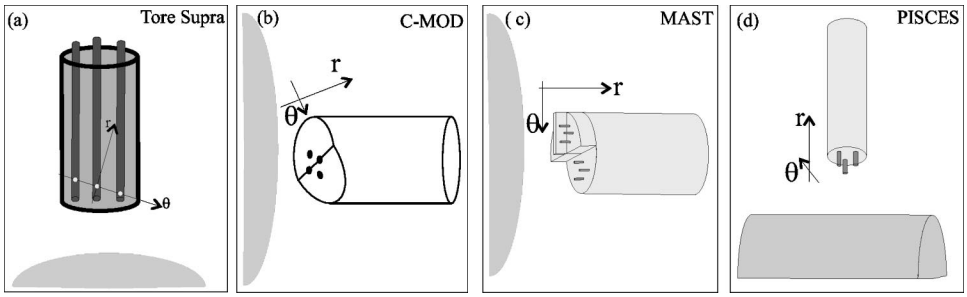

FIG. 1. A schematic of the four Langmuir probes used. (a) In Tore Supra the tips are protected by a cylinder with a 3 cm diameter. Holes are drilled through the protection cylinder defining the collection area. The holes diameter is 4 mm and the poloidal distance among the tips is 0.68 mm. (b) In Alcator C-Mod the tips are flushed on the probe surface. Their diameter is 1.5 mm and distanced poloidally by 3.8 mm. (c) In MAST the probe contains 9 tips with diameter 1.5 mm and a height of 1 mm. The poloidal separation is 4 mm and the radial separation is 0.5 cm. (d) In PISCES is used a simple configuration of three tips with 0.2 mm of diameter and a height of 1 mm. The poloidal distance is 0.5 mm.

B. The Alcator C-Mod tokamak

In contrast to Tore Supra, the separation between the plasma and the walls is achieved using a divertor in the Alcator C-Mod tokamak. The data that we are going to study were taken under the following plasma configuration: Magnetic field equal to 5.3 T, plasma density about 1×10^{20} m^{-3}, plasma current 0.8 MA, major radius 70 cm, and minor radius 21 cm. The deuterium discharges were ohmically heated with a single-lower null diverted equilibrium.[13] The distance between the LCFS and the walls is limited to few centimeters.

The reciprocating probe on Alcator C-Mod is positioned at 10 cm above the midplane on the low field side of the tokamak. However, no reciprocation is performed for the present study, so the probe position in the SOL is fixed as well as the plasma radius and position. The probe position to the LCFS is about 0.7 cm. The probe tips are positioned as indicated in Fig. 1(b). The distance between two poloidally separated tips is 0.38 cm. Each tip has a diameter of 0.15 cm. They are flush to the surface of the probe head from which they are isolated by a ceramic coating. Two probes are biased to the ion saturation current with a constant -200 V, and two probes are kept floating providing the measurement of the poloidal electric field.[14]

C. The MAST spherical tokamak

The Mega Ampère Spherical Tokamak (MAST) has been newly commissioned and newly operational.[15] MAST has an aspect ratio $\varepsilon=R/a$ about 1.4 ($R=0.73$, $a=0.52$) much smaller than conventional tokamaks such Tore Supra and Alcator C-Mod where ε is equal to 3.24 and 3.33, respectively. On the other hand, the plasma density, temperature, and current in the MAST are comparable to other tokamaks. The gas used for our study is deuterium, and the main plasma parameters are: magnetic field 0.6 T, plasma density 1.5×10^{19} m^{-3}, plasma current 0.7 MA. The plasma was ohmically heated. MAST does not have a first wall close to the plasma, therefore, one can look for avaloids far from the LCFS.

The tips setup on the probe head is schematized in Fig. 1(c). It is located at the outer midplane and contains three sets of tips. Each set contains three tips put in triple-probe mode providing density and temperature fluctuations measurement. The diameter of each tip is 0.15 cm and the poloidal distance among one set of tips is 0.4 cm. In the radial direction the distance between the two set of probes is 0.5 cm. The acquisition frequency is 1 MHz and the total number of points recorded for each tip is 180 000. For the data used here, the probe remained in the SOL with distances between 5 and 30 cm from the LCFS.

D. The PISCES linear device

Plasma in the PISCES linear device is maintained by hot electrons coming from a lanthanum–hexaboride (LaB_6) plate leading to a steady state reflex arc discharge.[16] The baffle tube and the axial magnetic field ($B=0.12-0.24$ T) limit the plasma radial extension. The baffle tube is centered on the axis of symmetry of the cylindrical plasma and has a radius of $r=2.5$ cm. The vessel wall is at a distance 10 cm from the plasma center. The electron density and temperature inside the main plasma column are about 4×10^{18} m^{-3} and 20 eV. Plasma properties are investigated by a three-tip Langmuir probe having each a diameter of 0.2 mm and poloidally separated by 0.5 mm. The middle tip records the ion saturation current (I_{sat}) and the other two the floating potential (ϕ). In this article, the working gas in PISCES is hydrogen.

III. THE PROBABILITY DISTRIBUTION FUNCTION

This section is dedicated to comparing the raw ion saturation signals and the probability distribution function (PDF) for the four plasma devices. Before showing the statistical properties of the four signals, we aim at giving the reader the opportunity to view the raw signals recorded in the SOL of the MAST, Alcator C-Mod, Tore Supra, and PISCES. In Fig. 2 is plotted the four raw signals normalized to the standard deviations so one can assess visually how much the spikes intensity exceeds the standard deviation values. The four signals show the same apparent behavior where they contain high frequency fluctuations on the top of an intermittent low frequency component. Avaloids signature, that is high intensity spikes, can be rather easily distinguished in the four plots. We do not observe any negative component of the bursts in the SOL of the four devices. Moreover, they look asymmetric in time, rising up abruptly and decaying rather

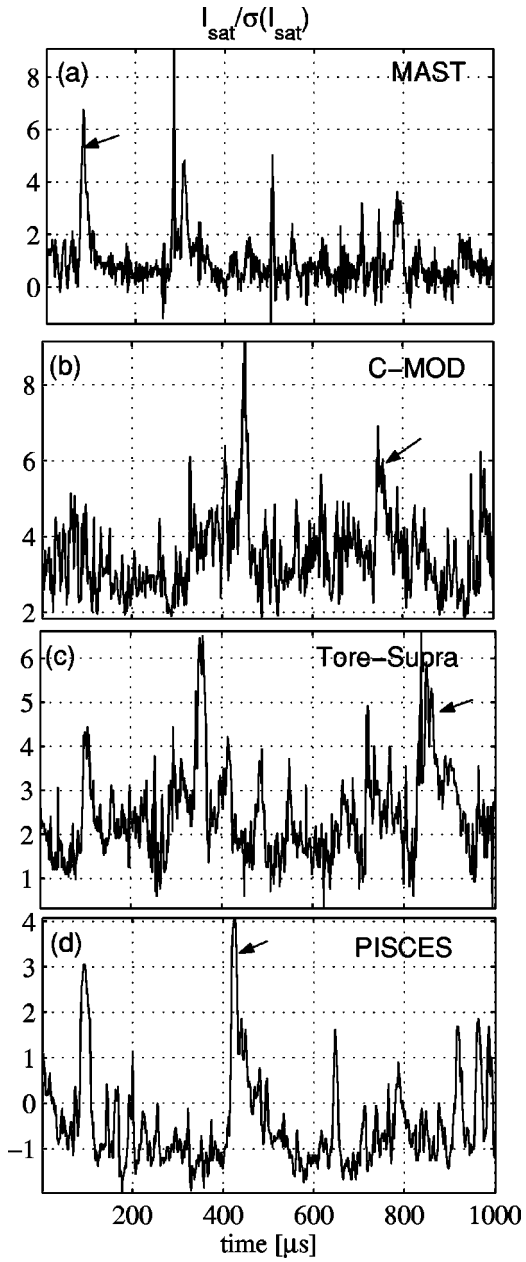

FIG. 2. The ion saturation current taken in the scrape-off layer of the four fusion devices MAST (a), Alcator C-Mod (b), Tore Supra (c), and PISCES (d). The arrows indicate the signature of avaloids.

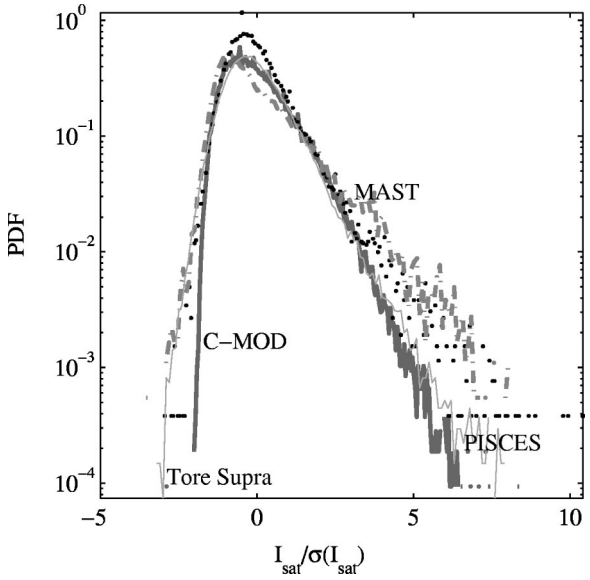

FIG. 3. A semilogarithmic plot of the PDF of the ion saturation current in the Tore Supra (solid line), Alcator C-Mod (thick solid line), MAST (dashed–dotted line), and PISCES (dots). The ion saturation current was normalized to the standard deviation and the integral of the four PDF is set equal to 1.

slowly. This fact is highlighted statistically after performing conditional averaging[6] and will be discussed hereafter. The other aspect common to the four time series is the same level of high frequency fluctuations inside and outside the spikes. This fact suggests that avaloids do not excite small scale fluctuations. The same argument was used in Ref. 7, where the high frequency component of the frequency spectra, reflecting turbulence small scales, decayed rapidly with an exponential law. On the other hand, the low frequency fluctuations, which reflect large turbulent scales, survived the parallel transport leading to plasma recorded even at 10 cm from the main plasma column center in PISCES.

Investigating the PDF's of turbulent fluctuations in general was emphasized by the Kolmogorov article, often called K41,[17] in which he assumed that fluctuations are random. Because the PDF of a random variable is Gaussian, it was rather straightforward to check this hypothesis by mainly using the normalized third and forth order moments of the fluctuating signal. For a signal denoted by x, the skewness factor is defined as $\langle x^3\rangle/\langle x^2\rangle^{3/2}$ and is equal to 0 for a Gaussian distribution reflecting its symmetry around the average value. The flatness factor is defined as $\langle x^4\rangle/\langle x^2\rangle^2$ and it can be considered as a measure of the weight of the tails of a distribution; it is equal to 3 for a Gaussian distribution. Townsend was one of the first to measure the PDF of the turbulent velocity field in a neutral fluid and obtained for the flatness factor a number close to 3, a value appropriate to a normal distribution.[18,19] In the SOL of magnetic confinement devices, it was reported by several authors that the PDF of the ion saturation current is not Gaussian reflecting the deviation from a normal distribution law. Figure 3 shows the PDF for the four confinement devices Tore Supra, Alcator C-Mod, MAST, and PISCES. They are normalized so that the PDF's integral is equal to 1, and the signals are normalized to their standard deviations. The features that were emphasized in Refs. 6 and 7 are reproduced for the four devices, namely:

(1) The part of the PDF that reflects negative density fluctuations decreases sharply with increasing intensity. Being in a semilogarithmic frame, this decrease indicates that the PDFs are very much close to a Gaussian distribution. Hence, the probability distribution function quantifies the visual inspection of the four raw signals where the positive spikes do not seem to have a negative density fluctuation component.
(2) The part of the PDF that reflects positive density fluctuations is highly non-Gaussian. The tails in a semilogarithmic frame decrease linearly reflecting an exponential

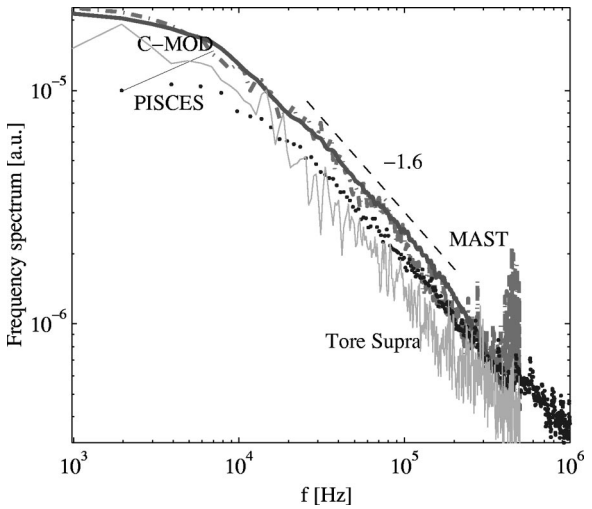

FIG. 4. A log–log plot of the power spectrum of the ion saturation current fluctuations in Tore Supra (solid line), Alcator C-Mod (thick solid line), MAST (dashed–dotted line), and PISCES (dots). The ion saturation currents, taken in the SOL, were normalized to the standard deviations.

law. The skewness and flatness factors of these curves are about 3 and 10, respectively, far from 0 and 3 for a Gaussian distribution.

We deduce that a visual inspection of the signal gives us some hints that the signals properties are similar for the four confinement devices. The PDF is one statistical tool that confirms this similarity.

IV. THE POWER SPECTRUM

The power spectrum (S), which is the Fourier transform of the second order correlation function, quantifies the correlation properties of a signal. For a white noise, the power spectrum has a flat featureless dependence on the frequency, indicating that there is no preferable frequency around which the fluctuation intensity occurs. On the other hand, a sine wave produces a narrow band peak indicating that all the fluctuations are occurring at the same frequency. For turbulence, Kolmogorov theory (K41) had a big impact on the way researchers investigated the correlation properties. The main advance was the assumption that, in the so-called inertial subrange, the correlation properties are self-similar leading to a power law dependence. It is for this reason that we plot in Fig. 4 the power spectra for the four confinement devices in a log–log frame. Another rather important aspect of turbulence power spectra is continuity. Landau assumed that power spectra is formed of an infinite number of fine lines each reflecting a mode.[20] But Ruelle and Takens showed that turbulence spectra can be continuous in the sense that only a few modes, because of their nonlinear interactions, can lead to a broadband spectrum.[21] The second concept of continuous spectrum was the one that was observed experimentally.[22]

In PISCES, the acquisition frequency is equal to 2 MHz, whereas in Alcator C-Mod and MAST and Tore Supra it is equal to 1 MHz. The four curves have the same correlation properties, namely:

(1) Only one scaling region is detected. This behavior indicates that the correlation is self-similar at least till the second order and that a description of the form $S \sim f^{\xi}$ is valid.
(2) The same scaling exponent describes the four power spectra, $\xi \simeq -1.6$.
(3) The power spectra contain very little high frequency fluctuations. All the measurements indicate that the power spectrum reflects instrumental noise for frequencies above 300 kHz.

We conclude that the correlation properties of the fluctuations in the four plasma devices are similar.

V. CONDITIONAL AVERAGING

Conditional averaging is a statistical tool used to select and study portions of a signal with some specific features. The selection criterion is dictated by the type of information that one wants to investigate. For our analysis, the intermittent bursts are chosen with respect to their amplitude. However, one can choose different aspects such as coherence or oscillation duration. The threshold above which the amplitude is selected is three times the standard deviation. For a random signal with a Gaussian distribution, only 0.13% would be encountered with amplitude greater than three times the standard deviation. For intermittent signals, we have shown in Ref. 6 that the dependence on the choice of the threshold is not crucial. As long as the threshold is selected above the standard deviation, the number of bursts selected is more or less the same because they appear intermittently with intensity much greater than the background.

Conditional averaging is achieved by first selecting the maxima above a certain threshold. The selection process can be made on the signal, its absolute value or one can put the signal to an arbitrary power. The reason we select the absolute value of the signal is not to bias our choice towards positive or negative high intensity events. In order to study the time dependence of these high intensity bursts, we record 50 data points about each maximum. This leads to a matrix of $100 \times N_{\max}$, where $N_{\max}$ is the number of maxima. In the selection, we make sure that maxima are separated by 50 data points so we do not favor artificially one burst with a lot of fluctuations.

Langmuir probes usually have several tips with some biased to the ion saturation current, some are floating or in a triple probe configuration. We select the ion saturation time series because we are interested in the bursts that transport relatively large amounts of particles. However, one can also choose for example the floating potential[23] or the radial velocity deduced from the difference between two poloidally separated floating tips. In the latter case, one would be looking at characterizing high velocity events.

Once the maxima are pin pointed, we define the ''auto-conditional averaging'' to indicate the case where the maxima selection and the averaging are performed on the same signal. On the other hand, ''cross-conditional averaging'' describes the case where the selection is made on one signal and the averaging is made on another.

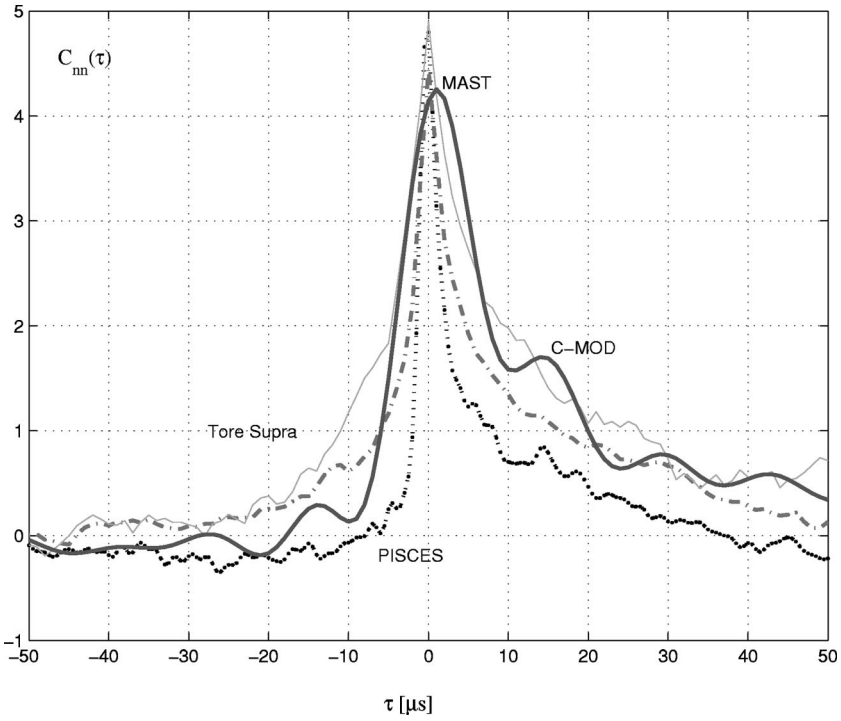

FIG. 5. The autoconditional average C_{nn} in Tore Supra (solid line), Alcator C-Mod (thick solid line), MAST (dashed–dotted line), and PISCES (dots).

In the above discussion, we indicated that there are several ways to use conditional averaging. It allowed us to justify the different choices that we made in order to analyze the turbulent signals in the SOL of the four fusion devices.

A. The average shape of an avaloid

As discussed earlier, the averaging over the number of maxima reduces the matrix to a vector with 100 elements that describes, on the average, the shape of the bursts and their intensity. Figure 5 shows the result of the autoconditional averaging C_{nn} for the four devices, Tore Supra, Alcator C-Mod, MAST, and PISCES; the indices nn indicates that the selection of the maxima was done on the density fluctuations and the averaging was performed on the density fluctuations. The data were normalized to the standard deviation of the overall signal. This figure clearly put forward the similarity of the avaloids signature on the ion saturation current that can be summarized in two points:

(1) Although in the selection no difference is made between positive and negative fluctuations, the four curves indicate that bursts are primarily composed of positive fluctuations. This is in agreement with the PDF of the four data strings which quantify this aspect and confirms that avaloids do not possess a negative fluctuation component.
(2) The curve in time shows asymmetry where an abrupt increase at negative times is followed by a longer decrease at positive times. This is indicative of the spatial shape of the avaloids which may be composed of a sharp front of matter followed by a long tail (like comets). In fusion plasmas this shape is often related to relaxation phenomena.

The above two main properties also suggest that the bursts are not coherent structures caused by coherent vorticity as it is encountered in neutral fluids. Coherent vortices lead to particle concentration around the core leading to negative as well as positive density fluctuations. Moreover, it leads to spatial symmetry around the core because of the rotation. Hence, intermittent structures in the SOL of magnetically confined plasmas are different from the ones found in neutral fluids.

B. Radial velocities and spatial scales

The autoconditional average describes the time signature of avaloids. In this section, we determine their radial velocity as well as their spatial dimension. In Ref. 7, we showed that in PISCES, avaloids velocity can reach 1500 m/s in the SOL. Among the four devices, we were able to determine the avaloids radial velocity (V_r) in MAST, Alcator C-Mod, and PISCES. In C-Mod and PISCES, V_r is determined as E_θ/B_T, where E_θ is the poloidal electric field measured from the difference of two poloidally separated floating tips. In MAST, V_r is calculated by cross-conditional averaging two radially separated tips biased to the ion saturation current. The results are plotted in Fig. 6. In Alcator C-Mod the radial average velocity is about 4×10^4 cm/s, whereas in PISCES, it is 1.5×10^5 cm/s. In MAST, the radial distance between the probes being 0.5 cm, and taking into account a shift of 5 μs, we obtain a radial velocity about 1×10^5 cm/s. These velocities can thus reach about 1/10th of the sound speed making this process of radial convection transport competitive with the parallel transport. Without this high radial velocity these structures could not survive the action of nearby walls and

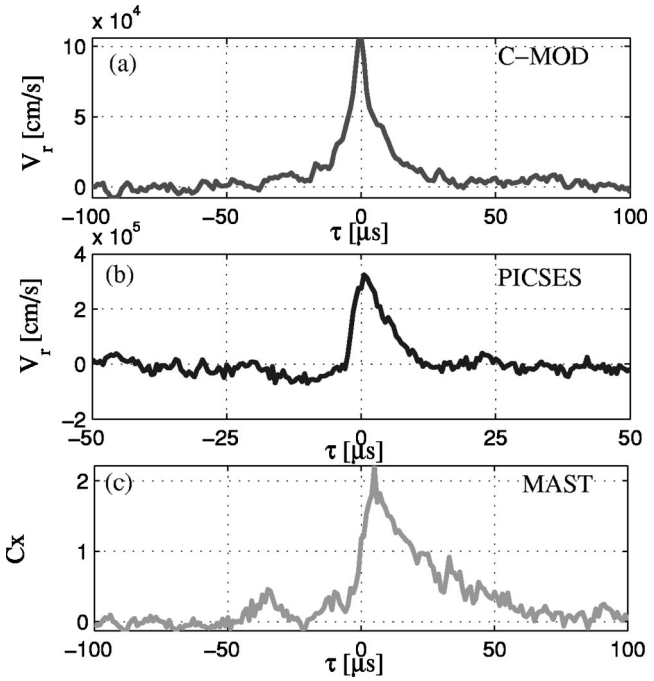

FIG. 6. (a) and (b) is the cross-conditional average in Alcator C-Mod and PISCES, respectively. The radial velocity is the $\boldsymbol{E}\times\boldsymbol{B}$ drift deduced from the difference of two poloidally separated tips. In (c) is shown the cross-conditional average in MAST where maxima are selected on one tip biased to the ion saturation current and the conditional averaging is performed on another tip, also biased to the ion saturation, but radially distanced by 0.5 cm.

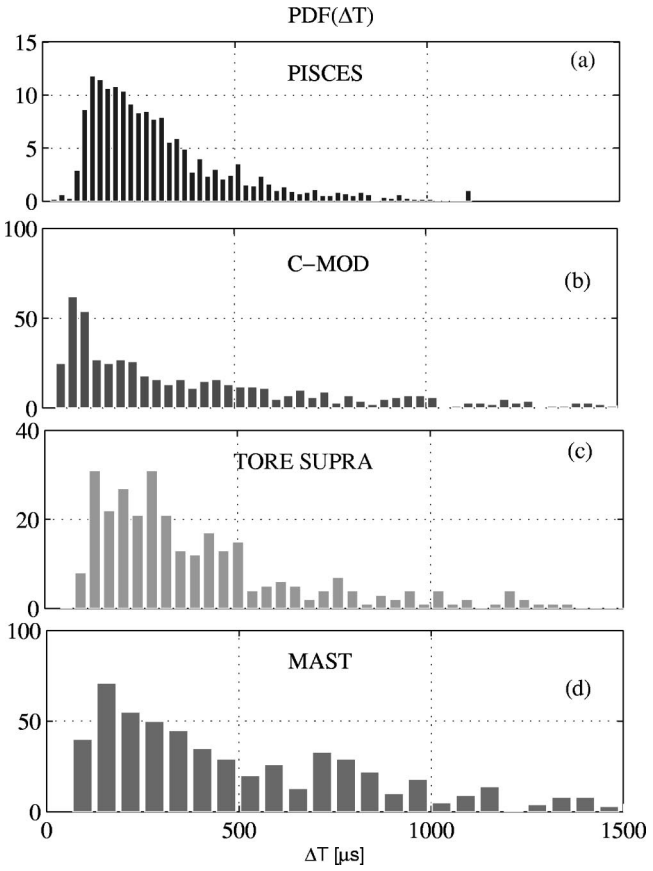

FIG. 7. The histogram of the times between two bursts for PISCES (a), Alcator C-Mod (b), Tore Supra (c), and MAST (d).

parallel transport. On the other hand, one can note the asymmetric shape of the V_r in agreement with that of the density fluctuations.

Having the three velocities, the radial length scales of avaloids are thus estimated at about $1/e$ of C_{nn} to be 4 cm in MAST, 1 cm in Alcator C-Mod, and PISCES. In addition to the magnetic configuration which might still play a role, the reason that the velocity and length scales of Alcator C-Mod are found smaller than in PISCES and MAST is probably caused by the vicinity of the walls to the plasma. This shortens the parallel connection lengths and thus enhances the parallel transport leading to a decrease of the avaloids poloidal and radial scales. The strong magnetic field of C-Mod may also play a role in setting the size of avaloids. In Tore Supra, we used the conditional average technique on three poloidally separated tips and obtained a poloidal velocity of avaloids about 5.7×10^3 cm/s and a poloidal length of 5.6 cm.[6]

C. The time between two bursts

Once the maxima are selected, one can determine the waiting time between two bursts ΔT and its PDF. Figure 7 shows the result of this operation conducted on the four plasma devices. The four PDF's have the following similar properties:

(1) The four devices present a PDF that is centered about a frequency of 200 μs. Consequently, the process behind the generation of avaloids may be periodic. This is actually in agreement with the avaloids shape which suggests some type of a relaxation phenomenon.
(2) The PDF is skewed towards larger ΔT's. This fact reflects intermittency where larger lapses between two bursts contribute in a significant manner to the PDF of ΔT.

One can show that when the graphs are plotted in a semi-logarithmic plot, the part of the PDF which is greater than the average value presents a linear behavior reflecting an exponential-type distribution.

D. On the relation between the waiting time and the amplitude

Relaxation phenomena can be periodic, such as sawteeth inside a tokamak, or SOC-type such as sand piles. One of the main properties of self-organized critical (SOC) phenomena is the relation between the waiting time and the amplitude of the avalanche.[24] In other words, due to some type of friction, there is a build up of the profile until some critical gradient. Once this local gradient is steeper than the critical one, an avalanche is ejected. Because the gradient is everywhere critical the avalanche rolls all the way down the slope until it reaches a place with a shallower gradient. In such a phenomenon there is a close relationship between the waiting time

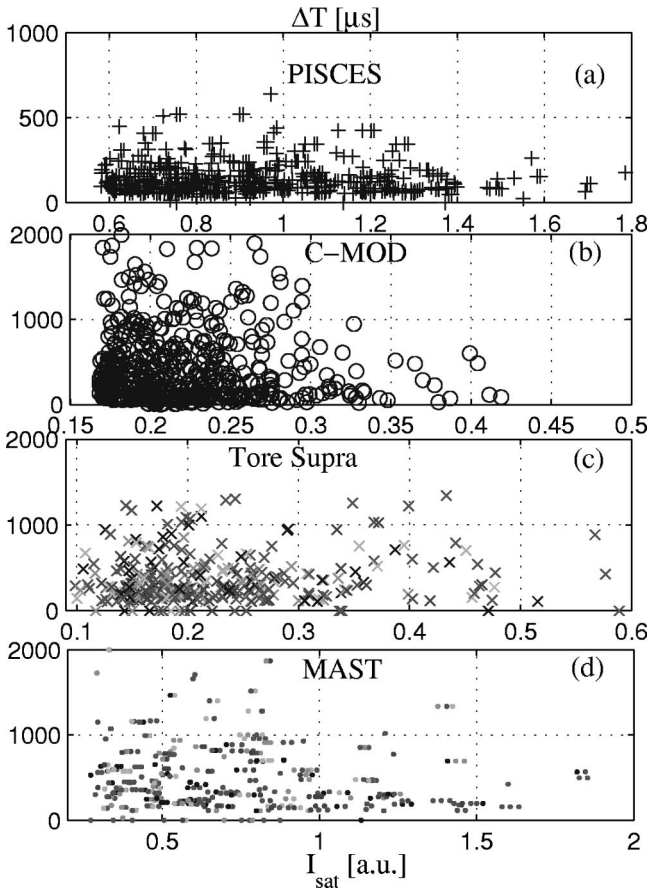

FIG. 8. For PISCES in (a), Alcator C-Mod in (b), Tore Supra in (c) and MAST in (d), is plotted the time between two bursts with amplitude greater than three times the standard deviation as a function of the bursts intensity.

and the avalanche amplitude. In contrast to the SOC, in a periodic type of relaxation no relation is expected between the waiting time and the amplitude.

In fusion, SOC models were proposed to explain the discrepancies between theory and experiment.[25] Some features of this model were supported by experiments using the power spectra.[26] However, many different mechanisms may lead to a $1/f$ type of spectrum and, on the other hand, many SOC-type phenomena lead to power spectra different from $1/f$. Hence, and as it was concluded in Ref. 6 one should compare not only the power spectrum but also other properties. In the present article, the power spectra did not show in the four devices a $1/f$ scaling region. This fact should not be interpreted as an argument against the SOC phenomenology as we just indicated above.

But being able to pin point the maxima above a certain threshold, one can relate the time between bursts to the amplitude of the burst. This is plotted in Fig. 8 for the four devices. It is rather clear that there is no relation between ΔT and the bursts amplitude. A SOC-type phenomenon would lead to data points aligned along a line with some nonvanishing slope. Consequently, we deduce that the process underlying avaloids is not of SOC-type. This is true for at least MAST, Alcator C-Mod, Tore Supra, and PISCES.

Using the conditional averaging technique, we put forward the similarity of the temporal properties of avaloids in the four plasma devices MAST, Tore Supra, Alcator C-Mod, and PSICES. This is reflected in the shape of the auto-conditional average as well as in the waiting time distribution. We also showed that in Alcator C-Mod, PISCES, and MAST the radial velocity of avaloids can reach 1/10th of the sound speed. Finally we showed that there is no relation between the waiting time and the amplitude. This suggests that origin of avaloids is most probably not of the SOC-type.

VI. MAST PROFILES

In PISCES avaloids are detected at the wall, that is, at 7.5 cm far from the plasma edge.[7] In Fig. 9(a), we show that this is also the case for MAST spherical torus where plasma is detected up to 30 cm away from the LCFS. The average ion saturation current dependence on the distance r to the LCFS is shown in Fig. 9(b), and can be approximated by an exponential decay with $\lambda_{\mathrm{SOL}} \simeq 1.6$ cm. However, this approximation is valid only until $r \simeq 9$ cm and cannot reproduce the profile which extends at least twice as far. One should recall that MAST does not have a first wall that can produce a sink for particles. This leads to avaloids radial propagation without significant losses due to short parallel connections. Hence, the profile should be rather flat which is the case as indicated in Fig. 9(b).

The main conclusion one can draw is that in MAST spherical torus, as in PISCES linear device, plasma is detected in an intermittent fashion at distances far from the last closed flux surface. This distance can be several 10's of centimeters depending on the existence or not of first walls that enhance parallel transport by reducing the parallel connection lengths.

VII. CONCLUSION

The purpose of this article is to investigate the universality of convective turbulence in the scrape-off layer of magnetically confined plasmas. The four chosen devices are different in many ways. MAST is a spherical tokamak while Alcator C-Mod is a conventional tokamak. The difference between Alcator C-Mod and Tore Supra is the way plasma is being kept away from walls, diverted in the first limited in the second. Finally PISCES differs from all the other three by being a linear device with no closed field lines and no curvature.

The comparison among the different turbulent signals was performed using different statistical analyses. The reason behind using several signal processing schemes is to show that the signals are identical in many different ways. First, we used the raw time traces of the ion saturation currents which, at least visually, showed that the four time series are similar containing high frequency fluctuations in addition to a low frequency component that reflects avaloids. The probability distribution function was the first statistical tool used for comparison. The same features were recorded on the four signals, that is, positively skewed graphs with a Gaussian negative density fluctuations. The power spectra were shown to be similar reflecting the same correlation properties. This was reflected in the same scaling exponent of only one scaling region. The use of the conditional averaging re-

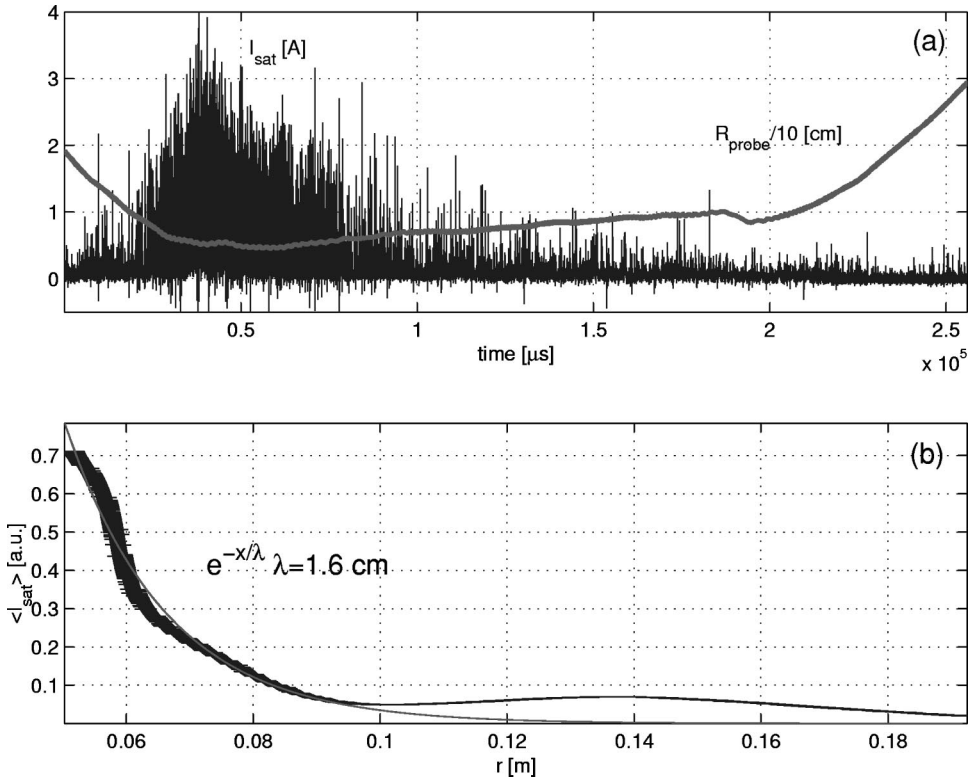

FIG. 9. (a) The ion saturation current as function of time in MAST. Also is shown the probe motion during the same time indicating that the probe moved as close as 5 cm to the LCFS (thick solid line). (b) The radial average profile and the fit by an exponential law leading to $e^{-x/\lambda}$, where λ is about 1.6 cm. Note that this determination is calculated with a radial offset of 5 cm.

vealed the same average temporal signature of avaloids for the four devices. We recorded an abrupt increase of the density followed by a rather slow decrease. This fact provides hints that the generation process may be a relaxation phenomenon. The idea that this relaxation phenomenon is of the SOC type is undermined by the experimental finding that the amplitude of the fluctuation does not depend on the waiting time. The histogram of the time between two bursts is shown to be similar as well with a rather central frequency and positively skewed distribution. For the four devices the value of the central frequency is almost the same about 200 μs. From the conditional averaging, we determined the avaloids radial velocities and radial length scales. The velocities were found to be high ranging from 500 m/s in Alcator C-Mod to 1000 m/s in MAST.

Toroidal geometry does not seem to be a necessary condition for the existence of avaloids because they are detected in toroidal as well as linear devices. This conclusion, however, should not be interpreted as the curvature drift does not lead to avaloids generation or does not play a role in avaloids propagation. As a matter of fact, the curvature drift or centrifugal forces are equivalent to the gravitational force in the sense that they can all lead to a Rayleigh–Taylor type of instability.[27] Accordingly, while in tokamaks, avaloids generation as well as propagation might be dominated by the curvature drift,[28] in linear devices another equivalent force, such as the centrifugal force, might play this role leading to the same dynamics in the SOL as reported here. Hence, the fact that turbulence properties are the same in linear and toroidal devices does not allow us to conclude whether the curvature effects dominate or not avaloids dynamics. In order to have a clearer picture about the importance of different processes, two additional investigations should be undertaken: First, is linear stability analysis and detailed simulation of the plasma edge including the scrape-off layer. This should help identifying the type of instability that is taking place. Second, are parametric dependencies of the turbulence properties, where one can take advantage of the fact that different forces depend on different plasma parameters. This is the case for example of the temperature for the curvature drift and the poloidal velocity for the centrifugal force. One advantage that can be deduced from the analyses of this paper is that models and simulations of this process can be easier accomplished as simple geometry can be used.

We also showed that in MAST, plasma is detected to exist in bursts even at 30 cm away from the last closed flux surface. The same type of profile was shown in PISCES where plasma was detected in bursts as far as 10 cm (plasma radius equal to 2.5 cm).

The present comparison was made not only on different magnetic confinement devices but also using different probe designs. The dimensions of the probe scan from rather big in Tore Supra to very small in PISCES. The present investigation shows that the probe perturbation is not responsible for the bursts generation and does not alter significantly turbulence properties in the scrape-off layer. It is often admitted that probe perturbation of turbulence occurs and may be significant at scales equal and smaller than the probe dimension. But on the other hand, turbulence spatial scales are integrated over the probe scale. Consequently, the perturbation cannot be detected because while the probe perturbs small scales, it also averages over them. So, as long as turbulence with scales larger than the probe is investigated, the properties of the fluctuations are little affected. Further investiga-

tion is required about the probes effects on the absolute values of transport as it was discussed in Ref. 14.

The detailed study presented in this article showed that intermittent convective transport by intermittent large-scale high-velocity events, called avaloids, is universal in the sense that it is encountered in most toroidal as well as linear plasma devices leading to identical properties of turbulent fluctuations in the scrape-off layer.

ACKNOWLEDGMENTS

G.A. would like to thank S. I. Krasheninnikov for fruitful discussions.

This work was performed under the U.S. Department of Energy Contract Nos. DE-FG03-95ER-54301 and DE-FC02-99ER54512 and was jointly funded by Euratom and U.K. Department of Trade and Industry. Y.Y. would also like to acknowledge a grant from the British Royal Society.

[1]S. J. Zweben and R. W. Gould, Nucl. Fusion **25**, 171 (1983).
[2]R. Jha, P. K. Kaw, S. K. Mattoo, C. V. S. Rao, Y. C. Saxena, and ADITYA Team, Phys. Rev. Lett. **69**, 1375 (1992).
[3]M. Endler, H. Niedermayer, L. Giannone, E. Kolzhauer, A. Rudyj, G. Theimer, and N. Tsois, Nucl. Fusion **35**, 1307 (1995).
[4]R. A. Moyer, R. D. Lehmer, T. E. Evans, R. W. Conn, and L. Schmitz, Plasma Phys. Controlled Fusion **38**, 1273 (1996).
[5]B. LaBombard, M. V. Umansky, R. L. Boivin *et al.*, Nucl. Fusion **40**, 2041 (2000).
[6]G. Antar, P. Devynck, X. Garbet, and S. C. Luckhardt, Phys. Plasmas **8**, 1612 (2001).
[7]G. Y. Antar, S. I. Krasheninnikov, and P. Devynck, Phys. Rev. Lett. **87**, 065001 (2001).
[8]P. C. Stangeby, *The Plasma Boundary of Magnetic Fusion Devices* (IOP, London, 2000).
[9]H. Maier, K. Krieger, M. Balden, J. Roth, and the ASDEX Upgrade Team, J. Nucl. Fusion **266-269**, 1003 (1999).
[10]ITER Physics Experts Groups on Confinement and Transport and Confinement Modeling and Database, Nucl. Fusion **39**, 2175 (1999).
[11]Equipe Tore Supra (prepared by F. Saint Laurent), Nucl. Fusion **40**, 1047 (2000).
[12]J. P. Gunn, Phys. Plasmas **8**, 1040 (2001).
[13]B. LaBombard, R. L. Boivin, and M. Greenwald, Phys. Plasmas **8**, 2107 (2001).
[14]B. LaBombard, Phys. Plasmas **9**, 1300 (2002).
[15]A. Sykes, J.-W. Ahn, and R. Akers, Phys. Plasmas **8**, 2101 (2001).
[16]D. M. Goebel, G. Campbell, and R. W. Conn, J. Nucl. Mater. **121**, 277 (1984).
[17]A. N. Kolmogorov, C. R. Acad. Sci. URSS **30**, 301 (1941).
[18]A. A. Townsend, Proc. Cambridge Philos. Soc. **43**, 560 (1947).
[19]G. K. Batchelor, *Homogeneous Turbulence* (Cambridge University Press, Cambridge, 1970).
[20]L. D. Landau and E. M. Lifshitz, *Fluid Mechanics* (Pergamon, London, 1968).
[21]D. Ruelle and F. Takens, Commun. Math. Phys. **20**, 499 (1971).
[22]H. G. Schuster, *Deterministic Chaos* (VCH, Germany, 1988).
[23]A. V. Filippas, R. D. Bengston, G.-X. Li, M. Meier, Ch. P. Ritz, and E. J. Powers, Phys. Plasmas **2**, 839 (1995).
[24]H. J. Jensen, *Self-Organized Criticality* (Cambridge University Press, Cambridge, 1998).
[25]P. H. Diamond and T. S. Hahm, Phys. Plasmas **2**, 3640 (1995).
[26]R. A. Moyer, K. H. Burrell, and T. N. Carstrom, Phys. Plasmas **2**, 2397 (1995).
[27]F. F. Chen, *Plasma Physics and Controlled Fusion* (Plenum, New York, 1984).
[28]S. I. Krasheninnikov, Phys. Lett. A **283**, 368 (2001).